Journal of Magnetics 10(4), 163-170 (2005)

RF Integrated Electromagnetic-Noise Filters Incorporated with Nano-granular $Co_{41}Fe_{38}Al_{13}O_8$ Soft Magnetic Thin Films on Coplanar Transmission Line

Jae Cheon Sohn[1]*, Masahiro Yamaguchi[2], Sang Ho Lim[3], and Suk Hee Han[1]

[1]*Future Technology Division, Korea Institute of Science and Technology, P. O. Box 131, Cheongryang, Seoul, 130-650, Korea*
[2]*ECEI Department, Tohoku University, Sendai 980-8579, Japan*
[3]*Department of Materials Science and Engineering, Korea University, Seoul 136-701, Korea*

(Received 16 November 2005)

The RF integrated noise filters are fabricated by photolithography. The stack for the electromagnetic noise filters consists of the nano-granular ($Co_{41}Fe_{38}Al_{13}O_8$) soft magnetic film / SiO_2 / Cu transmission line / seed layer (Cu/Ti) / SiO_2-substrate. A good signal-attenuation feature along with a low signal-reflection feature is observed in the present filters. Especially in the noise filter incorporated with a $Co_{41}Fe_{38}Al_{13}O_8$ magnetic film with lateral dimensions of 2000 μm wide, 15 mm long and 1 μm thick, the maximum magnitude of signal attenuation reaches −55 dB, and the magnitude of signal reflection is below −10 dB in the overall frequency range. And this level of signal attenuation is much larger than that of a noise filter incorporated with a Fe magnetic film.

Key words : nanogranular soft magnetic film, electromagnetic noise filter, low pass filter, L-C resonance, ferromagnetic resonance

1. Introduction

Harmonics in power circuits are frequencies that are integer multiples of a fundamental frequency generated by non-linear electrical and electronic equipment [1]. The term nonlinear load is commonly used to describe the switch mode power supply, including all active devices composed of transistors or diodes, found in personal computers and mobile phones. The fundamental frequency combines with the harmonic sine waves to form repetitive, non-sinusoidal distorted wave shapes, causing the different frequencies to flow back on the electrical system, even though they do not perform any useful work. These frequencies reduce current capacity on the wiring system, cause overheating of electrical apparatus, and even disturb normal voltages when the interaction is extreme. And also, serious electromagnetic wave interference causing dysfunction in electronic devices is aroused by the harmonics. As problems caused by nonlinear loads become increasingly obvious, the effort to decrease the effects of nonlinear loads on their facilities has been demanded. This study discusses the possibility of the integrated countermeasure of RF electromagnetic noise emission on an RF integrated coplanar waveguide (CPW) transmission line by using loss generation of both nano-granular soft ferromagnetic thin films and insulating thin films. The main mechanism of the loss generation is L-C resonance which is taken place by the combination of the distributed inductance of magnetic film and the distributed capacitance of insulating film. In addition to the L-C resonance loss, two minor loss components should be considered, which are generated by eddy current and ferromagnetic resonance (FMR) losses [2]. The coplanar waveguide transmission line basically has a pass-band that covers the signal frequency range. Without the magnetic film, the noise harmonics of the signal pass through the transmission line with only a little attenuation. The ideal role of magnetic film is not to raise insertion losses in the pass band but to give as large attenuation as possible to eliminate the noise harmonics at the stop-band. This operation is possible by either power reflection at the input end of magnetic film or power losses in the magnetic and insulator films. The primary concern with the magnetic thin film is to have large loss generation in a high-frequency range, especially in the gigahertz frequency range where most of the bulk

*Corresponding author: Tel: +82-2-958-5427,
Fax: +82-2-958-6851, e-mail: jcsohn@kist.re.kr

and the composite ferrite materials have only a small loss generation. So, firstly in this study, electromagnetic noise filters are fabricated on a coplanar transmission line incorporated with nano-granular Co-Fe-Al-O soft ferromagnetic thin films. It has been proved by the authors that the nano-granular Co-Fe-Al-O soft magnetic films have a large uniaxial anisotropy field (H_K), a high electrical resistivity (ρ), and an excellent soft magnetic feature [3, 4]. And finally, the signal attenuation and reflection characteristics of these noise filters are analyzed to determine the possibility of application to the low-frequency-pass filters with a wide stop-bandwidth.

2. Experimental

The coplanar waveguide (CPW) transmission line with a characteristic impedance of 50 Ω is designed with a 50-μm-wide and 3-mm-thick signal line on the 7059 corning glass (permittivity, ε_r = 5.84) substrate, which is calculated using Muller and Hilberg equation [5]:

$$Z_0 = \frac{\eta_0}{4.0\sqrt{\varepsilon_{eff}}} \frac{1}{[K(k_1')/K(k_1)] + (t/b - a)} \quad (\Omega)$$

$$\varepsilon_{eff} = 1 + \frac{\varepsilon_r - 1}{2} \frac{K(k_1')/K(k_1)}{[K(k_1')/K(k_1)] + (t/b - a)}. \quad (1)$$

The characteristic impedance Z_0 and effective permittivity of the coplanar line ε_{eff} are given as the above equation. The Z_0 = 50 Ω line was, thus, designed with a = 50 μm, b = 70 μm, c = 400 μm, and t = 3 μm on the glass substrate as shown in Fig. 1(a). The k_1, k_1', k_2, and k_2' are the functions of cross-sectional dimensions of a, b, c and t. As shown in Fig. 1(a) and (b), the structure of RF noise filter is composed of the stack of magnetic film (1 μm)/SiO_2 (0.1 μm)/Cu transmission line (3 μm)/glass substrate (1 mm), which was fabricated by the micro fabrication process. The Cu/Ti seed layers with the thickness of 0.06 and 0.01 μm, respectively, are deposited by RF sputtering. The Cu transmission lines were deposited by electroplating method with an electrolyte composed of $CuSO_4$, H_2SO_4 and DI water. Then, the seed layers were etched by ion milling after removing the photo-resist frame for Cu transmission lines.

The amorphous $Co_{41}Fe_{38}Al_{13}O_8$ magnetic films ($4\pi M_S$ = 12.9 kG, H_K = 50 Oe, ρ = 374 $\mu\Omega$cm, f_R = 2.24 GHz) are deposited by RF magnetron sputtering on Ti/SiO_2 layer. To obtain well-aligned magnetic spins for the increment of H_K, magnetic films were deposited in the static magnetic field of 1 kOe. In order to improve the adhesion between the magnetic film and insulator layer, i.e., SiO_2 layers, Ti (~10 nm) was deposited on SiO_2 layers. After photo-resist patterning, the magnetic films were etched by

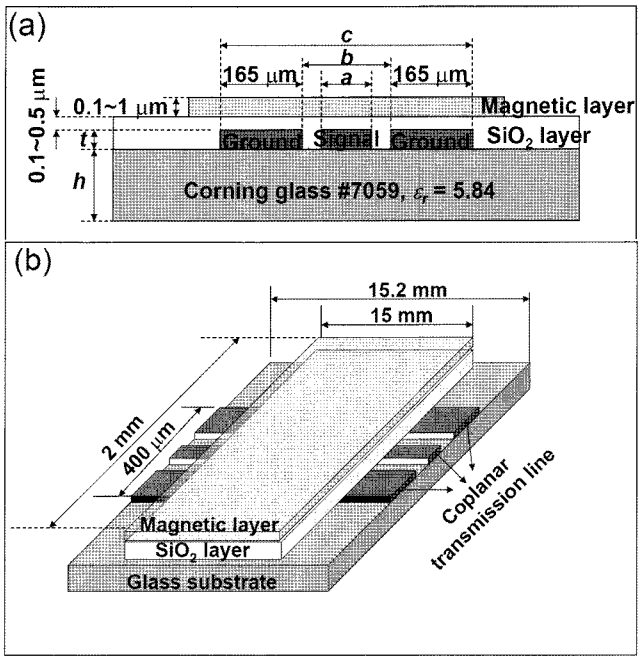

Fig. 1. (a) Cross-sectional view of the RF noise filter on coplanar transmission line. (b) Schematic presentation of the RF noise filter on coplanar transmission line.

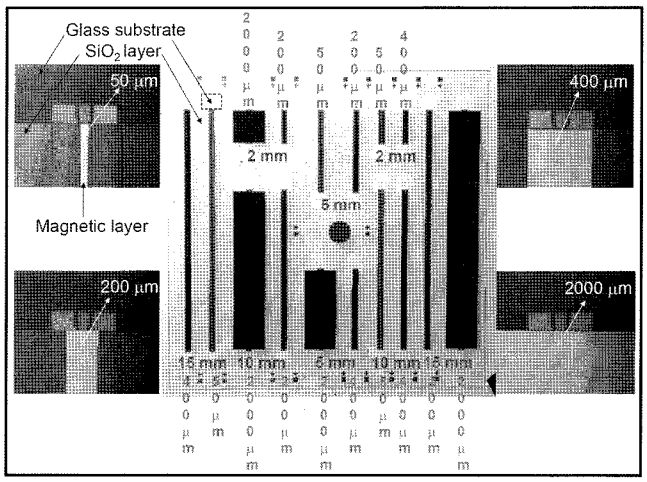

Fig. 2. Top view of the RF integrated noise filter with the change of the magnetic film's width from 50 to 2000 μm.

ion milling. To remove the SiO_2 layer on the contact pad, the wet etching method using Buffered Oxide Etch 1:6 was used for etching. Fig. 2 shows the top view of the RF noise filter after opening the contact pad by the wet etching method. The high frequency performance from 0.1 to 20 GHz was measured with two ground-signal-ground (GSG) pins type wafer probes which were mechanically touched at the left- and right-most ends of the transmission line, combined with network analyzer (HP 8720D). Fig. 3 shows the photograph of the microprobe arrange-

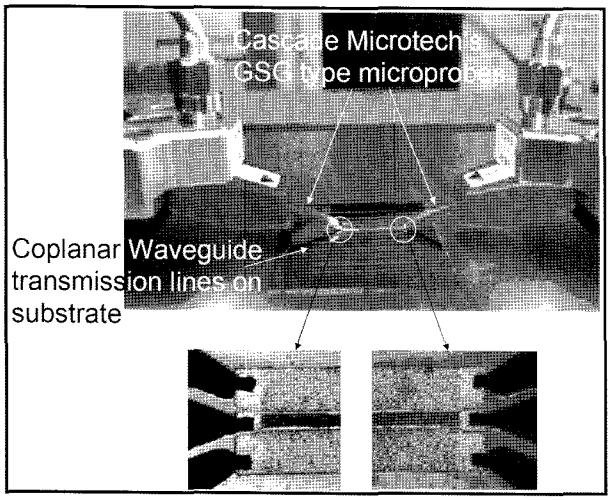

Fig. 3. Photograph of the measuring the integrated RF noise filter on the coplanar transmission line.

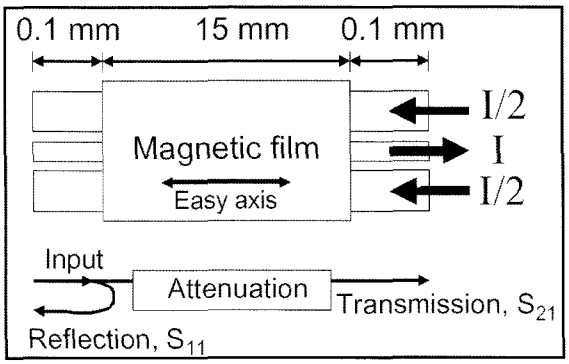

Fig. 4. A top view of a noise suppressor showing a magnetic film on top of the CPW transmission line. Note that the dimensions are not in a proper scale.

ment for measuring the integrated RF noise filter. A brief explanation of the *S*-parameters is given as follows (see Fig. 4). An input signal and/or noise is introduced from the left-hand side and is partly reflected at the left-hand end of the magnetic film. This reflected signal is called S_{11}, the reflection scattering parameter. The counterpart goes into the magnetic film portion where a certain degree of attenuation occurs mostly due to L-C resonance with minor eddy current and FMR losses. Then the transmission signal or noise, called the transmission scattering parameter (S_{21}), reaches the right-hand end of the CPW line.

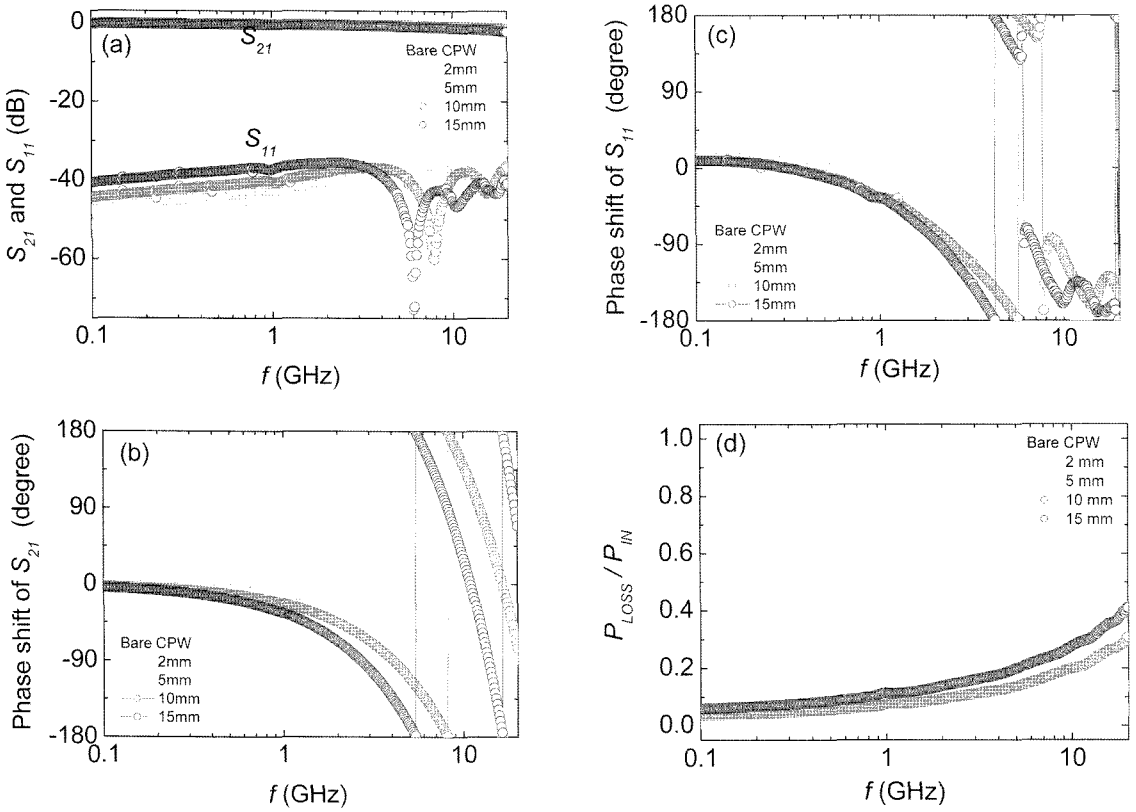

Fig. 5. (a) and (b). The frequency dependence of the transmitted (S_{21}) and reflected (S_{11}) scattering parameters (a) and the phase shift in S_{21} (b) of bare CPW transmission lines with the variation of the length. (c) and (d). Frequency dependence of phase shift in S_{11} (c) and power loss (d).

3. Results and Discussion

Fig. 5(a) shows the frequency dependence of the transmitted (S_{21}) and reflected (S_{11}) scattering parameters of bare CPW transmission lines with the variation of the length. In the frequency range being under 10 GHz, the signal attenuation of all samples takes place very little. In the frequency range being over 10 GHz, the signal attenuation takes place only a little, showing a little difference in the attenuation level in each sample. The transmitted signals on the 10-mm and 15-mm-long samples are a little more attenuated than those on 2-mm and 5-mm-long samples. The signal attenuation of the bare CPW line is due to the eddy current loss caused by its distributed inductance. In the low frequency range where the signal reflection (S_{11}) increases gently, the longer the sample is, the larger the reflection magnitude is. But this tendency changes quite oppositely in the high frequency range being over 4 GHz. The signal reflection pattern in this frequency range is more or less complicated; several minimum dips are observed (one minimum dip in 5 mm-long-sample, two minimum dips in 10 mm-long-sample, three minimum dips in 15 mm-long-sample). These minimum dips are thoroughly due to the dimensional resonance. The dimensional resonance in this case occurs when the half-wavelength of reflected signals is equal to the half-guided-wavelength. Figs. 5(b) and (c) show the frequency dependence of phase-shifts of the transmitted (S_{21}) and reflected (S_{11}) signals, respectively. The phase change in every 180° interval is found, showing the length-dependent feature. Fig. 5(d) shows the frequency dependence of the generalized power-loss of the samples. The generalized power-loss is calculated using the reflected (S_{11}) and transmitted (S_{21}) parameters as follows:

$$P_{loss}/P_{input} = 1 - (|S_{21}|^2 + |S_{11}|^2). \quad (2)$$

The power losses are the total losses occurring when the electrical signals pass along the CPW line. In the bare CPW line, the power loss is mainly due to the eddy current loss which is caused by the distributed inductance of the CPW line as mentioned above. The eddy current loss has a significant length-dependent feature in the high frequency range, since the distributed inductance of CPW line has the length-dependent feature.

Fig. 6(a) shows the signal attenuation with the magnetic-film width being from 50 to 2000 μm. The SiO_2 film of 0.1 μm thick is disposed as an insulating spacer between a coplanar transmission line and a magnetic layer. All magnetic layers have the equal length (15 mm) and thickness (1 μm). The signal attenuation increases

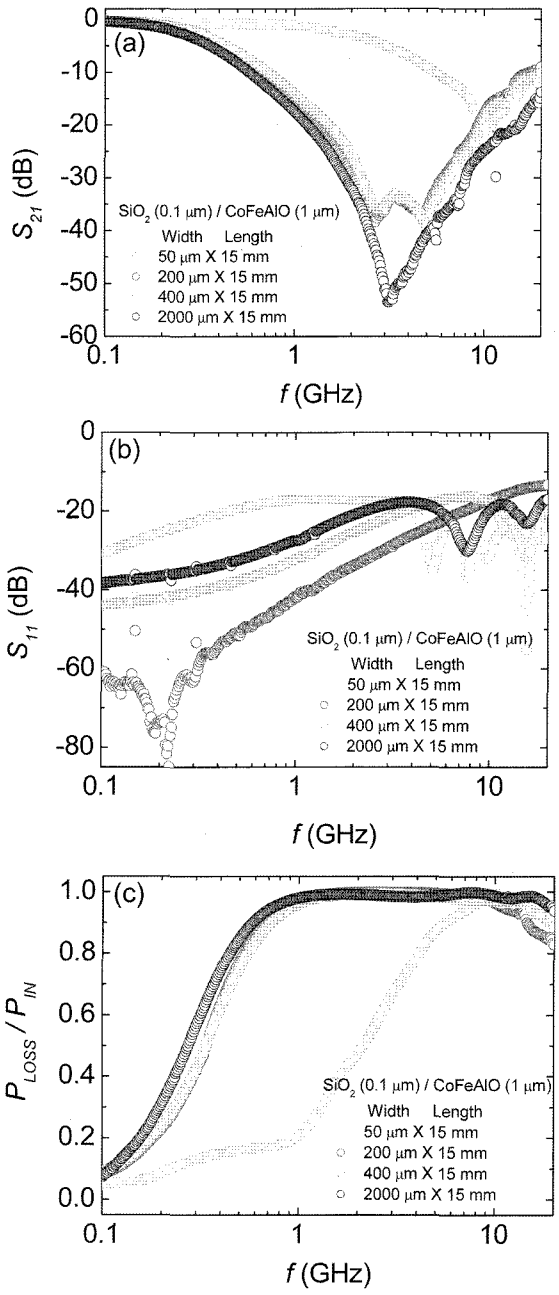

Fig. 6. (a) and (b). Signal attenuation (a) and reflection (b) with the change of the width of the magnetic film from 50 to 2000 μm (15-mm-long and 1-μm-thick magnetic film). (c). Power loss with the change of the width of the magnetic film from 50 to 2000 μm (15-mm-long and 1-μm-thick magnetic film).

with the width of insulating and magnetic layers in that both the distributed capacitance of insulating layer and the distributed inductance of magnetic layer increase with the width of both layers. So, the distributed capacitance and inductance become independent variables in determining the magnitude and frequency of the L-C reson-

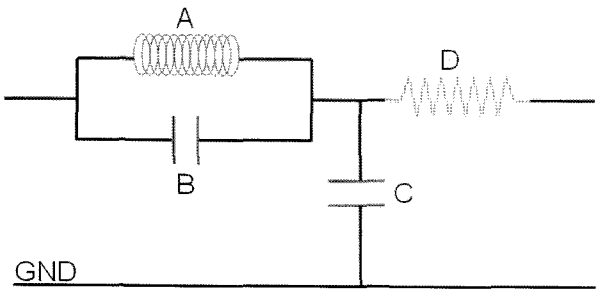

Fig. 7. Equivalent circuit of the coplanar transmission line incorporated with insulating and magnetic layers.

ance. The large minimum dips in the band-stop regions result from the large L-C resonance which causes a large level of signal absorption. In principle, the L-C resonant frequency shifts to the low frequency range with the values of the distributed capacitance and inductance in a high-frequency structure. This can be simply confirmed by the widely used equation $f_{LC} = 1/2\pi\sqrt{LC}$. And the magnitude of L-C resonance in a high-frequency structure also increases with the values of the distributed capacitance and inductance, since the impedance of the high-frequency structure increases with the values of both distributed elements. In practical, the bypass capacitive elements in high-frequency circuit structures increase the values of the impedance of the structures. Fig. 7 shows a parallel circuit structure which is the equivalent circuit of the present coplanar transmission line incorporated with insulating and magnetic layers. In this circuit, the elements A and B denote the distributed inductance of the magnetic-film incorporated coplanar-transmission-line and the distributed capacitance of the insulating layer, respectively. These two distributed elements couple each other in a certain frequency band and hence generating L-C resonance. The capacitor C is the other distributed element of the insulating layer but acts as a different role from the element B. In the high frequency range the distributed capacitor C provides a bypass on both ground-lines for a transmitted signal, causing a large capacitance loss. And the element D denotes the characteristic impedance 50Ω of coplanar transmission line.

Again in Fig. 6(a), the signal attenuation magnitudes of all samples except the 50-μm-wide magnetic film are nearly the same, indicating that the signal attenuation on the samples with magnetic layers of 200 μm wide and over rather saturates at a certain value than significantly increases. This saturation in signal attenuation is due to the fact that the effective approaching width of RF magnetic field by coplanar transmission line to the magnetic film is only about 200 μm. The maximum peak absorption of the microwave power is found at the L-C resonant frequencies: −55 dB at 3 GHz for the sample with 2000-μm-wide Co-Fe-Al-O layer, −40 dB at 4 GHz for the samples with 200 and 400-μm-wide Co-Fe-Al-O layers and −20 dB at 10 GHz for the sample with 50-μm-wide Co-Fe-Al-O layer. The samples with 200, 400 and 2000-μm-wide Co-Fe-Al-O layers show excellent attenuation features for practical applications to low-frequency pass-band filters with wide stop-bandwidth being from 300 MHz to 20 GHz. The CPW line with the 50-μm-wide Co-Fe-Al-O layer is also applicable to a low-frequency pass-band filter with a rather narrow stop-bandwidth being from 2 GHz to 20 GHz. The values of signal reflection of all samples shown in Fig. 6(b) are less than −10 dB which is low enough for filter applications. The reflection level −10 dB becomes $10^{-10/20}$ (= 0.316) when converted into the original normalized value by using Eq. (3).

$$S_{11} = 20\log\left(\frac{reflected\ voltage}{input\ voltage}\right). \quad (3)$$

The normalized value 0.316 means that 31.6% of the input signals do not reach the output port of transmission line. These non-transmitted signals are mostly reflected into the input port of transmission line. In general, it is widely accepted that the signal reflection value should be less than −10 dB for the frequency band-filter applications. When the signal reflection value is over −10 dB, the wave-form of the newly incoming input signal can be distorted by the synthesis with the reflected signal. The input signal modification due to the signal reflection commonly generates the serious dysfunction in electrical circuits. So the level of signal reflection should be maintained under −10 dB for efficient filter applications. Fig. 6(c) shows the generalized power losses of the samples with the width of the insulating and magnetic layers. In all samples except one with 50-μm-wide Co-Fe-Al-O layer, the plateau bands with 100% power-loss are observed from 1 GHz to 20 GHz. These large power-loss features with wide plateau bands are very unique as compared with those of other samples previously reported by other authors [6, 7]. The previously reported samples show the maximum peaks, not the wide plateau band, with about 80~90% power loss in their frequency profiles. It can be said that the present samples have larger wide-band L-C resonance losses than those of the previously reported samples.

In Fig. 8(a), the signal attenuation feature of the present sample incorporated with a Co-Fe-Al-O magnetic film is compared with those of other samples incorporated with two different magnetic layers Ni-Fe-Al-O and Fe. All magnetic layers have equal lateral dimensions 1 μm thick,

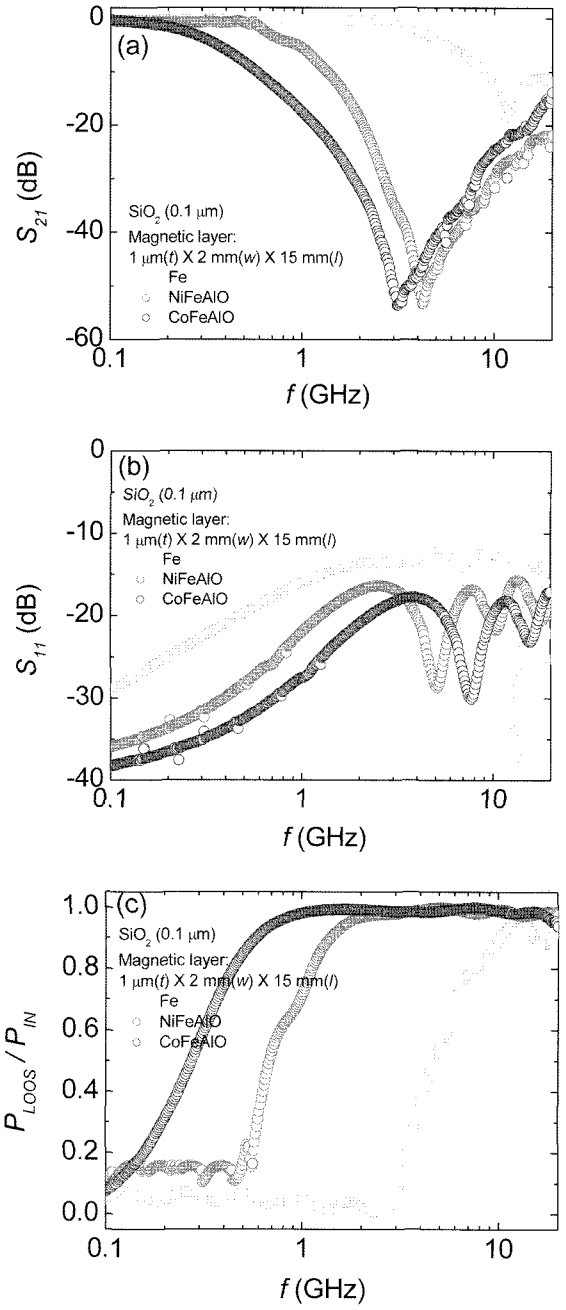

Fig. 8. (a) and (b). Frequency dependence of S_{21} and S_{11} for the present CPW transmission line with the 15-mm-long, 2-mm-wide, and 1-μm-thick Co-Fe-Al-O thin film, mainly to compare the present results with those for other CPW lines with 15-mm-long, 2-mm-wide, and 1-μm-thick Fe and Ni-Fe-Al-O magnetic films. (c) Frequency characteristics of the power losses of three samples.

2 mm wide and 15 mm long. And SiO_2 film of 0.1 μm thick is disposed as an insulating layer between a coplanar transmission line and a magnetic film. The transmitted signal on the coplanar line with Fe film is not attenuated much; about –20 dB at 11.5 GHz with a rather narrow stop-bandwidth being from 4.3 GHz to 20 GHz. In contrast, the other two samples show the large signal attenuation with wide stop-bandwidth. A sample incorporated with a Ni-Fe-Al-O magnetic film has maximum attenuation –55 dB at 4.5 GHz. This attenuation magnitude is exactly same as that of the sample with a Co-Fe-Al-O magnetic film. But the frequency at which the maximum attenuation (L-C resonance) occurs is not in correspondence to that of the sample with a Co-Fe-Al-O magnetic film. And also the sample with Ni-Fe-Al-O film shows a little narrower stop-bandwidth being from 600 MHz to 20 GHz. However, the sample with Ni-Fe-Al-O film has the very similar signal-attenuation tendency with the sample with a Co-Fe-Al-O magnetic film. The reason for this similar characteristic in signal attenuation is that the magnetic films of both samples have nano-granular structures where magnetic alloy nano-granules (Co-Fe and Ni-Fe) are embedded in an electrically insulating matrix phase (an amorphous Al-O oxide). This Al-O phase provides large capacitance for an entire nano-granular structure. The large capacitance of Al-O phase improves the total distributed capacitance of the sample, adding to the distributed capacitance of SiO_2 layer. And this improved capacitance combines with the inductance of magnetic alloy nano-granules and hence generating large L-C resonance at a certain frequency. On the other hand, a pure Fe material has large saturation magnetization and eddy current loss but does not have large capacitance. This is why the signal attenuation on the coplanar line with the Fe layer is not as large as that of the others with nano-granular magnetic layers. Fig. 8(b) shows the magnitudes of the signal reflection of three samples. The samples with nano-granular magnetic films have similar signal-reflection tendency each other as the signal-attenuation tendency observed in Fig. 8(a). The sample with Fe layer shows somewhat large reflection compared with the other samples. This large reflection is due to the large eddy current loss of the Fe magnetic layer. Fig. 8(c) shows the power losses of three samples. The sample with Ni-Fe-Al-O magnetic film shows a wide plateau band being from 2 GHz to 20 GHz. This plateau bandwidth is rather narrower than that of the sample with Co-Fe-Al-O magnetic film. In the sample with Fe film, a maximum power-loss peak appears at 12 GHz, which is mainly due to L-C resonance with minor eddy current and FMR losses.

A finite-element method (FEM) is applied to analyze the electromagnetic fields on coplanar transmission line by using the commercial simulation package (HFSS version 9.2.1). Figs. 9(a) and (b) represent the RF magnetic field distribution on the coplanar transmission line incorporated with and without magnetic and insulating films,

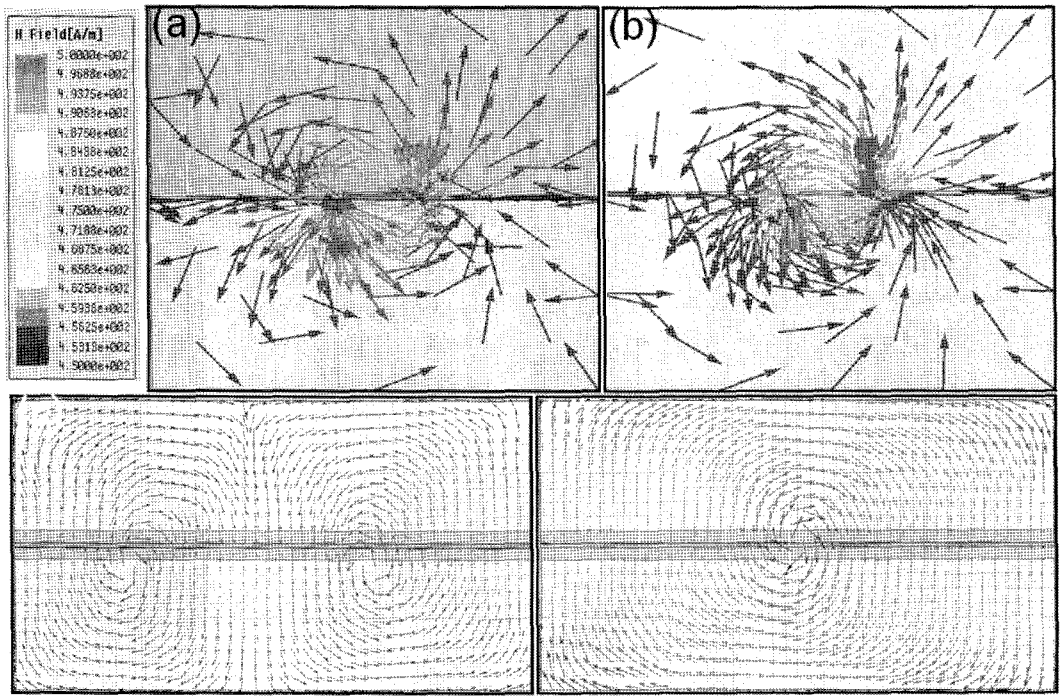

Fig. 9. (a)~(d). The cross-sectional views of RF magnetic fields at 20 GHz on CPW lines incorporated (a) with and (b) without magnetic and insulating layers. The top views of propagation of RF magnetic fields being in the near-field region on CPW lines (c) incorporated with and (d) without magnetic and insulating layers.

respectively. The magnetic and insulating films have equal lateral dimensions 3 μm thick, 50 μm wide and 2 mm long. The RF magnetic fields are depicted vectorially in the cross section at the output port of the bare CPW line. A large portion of the magnetic fields encircles the center conducting strip (the 50-μm-wide signal line), forming a closed-path with a diameter of 200 μm in a counterclockwise direction. Larger magnetic flux is observed in the bare CPW line than in the CPW line with magnetic and insulating layers, since the RF magnetic fields radiated from the CPW line with magnetic and insulating layers are reduced by the L-C resonance loss and two minor losses (the FMR and eddy current losses). But larger magnetic flux is *concentrated* around the center conducting strip of the CPW line incorporated with magnetic and insulating layers than of the bare CPW line. This is because the permeability of magnetic film gathers the magnetic flux around the center conducting strip. Figs. 9(c)~(d) depict the top views of propagation of the RF magnetic fields being in the near-field region. The magnetic flux makes a closed-path in a parallel direction with the top of the slots. The closed-path is formed at every half-wavelength of the propagating magnetic wave; one closed-path in the bare CPW line and two closed-paths in the CPW line with magnetic and insulating films. In the CPW line with magnetic and insulating films, the appearance of two magnetic-flux closed-paths means that the wavelength of RF magnetic wave is shortened during propagating along the transmission line.

4. Conclusion

The RF integrated noise filters are fabricated by photolithography. The stack for the electromagnetic noise filters consists of the magnetic layer / SiO_2 / Cu transmission line / seed layer (Cu/Ti) / SiO_2-substrate. The nano-granular $Co_{41}Fe_{38}Al_{13}O_8$ soft magnetic film with high uniaxial anisotropy and electrical resistivity is used as a magnetic layer in the noise filter. The signal attenuation on the transmission line is estimated by the *S*-parameters (S_{11}, S_{21}) up to 20 GHz. The L-C resonance is taken place by the coupling between the distributed inductance of the magnetic-film incorporated CPW-line and the distributed capacitance of the SiO_2 layer. Large signal attenuation (a minimum dip) appears at the L-C resonant frequency. Especially in the noise filter incorporated with a $Co_{41}Fe_{38}Al_{13}O_8$ magnetic film with lateral dimensions of 2000 μm wide, 15 mm long and 1 μm thick, the maximum magnitude of signal attenuation reaches –55 dB. And this level of signal attenuation is much larger than that of a noise filter incorporated with a Fe magnetic film. It can be concluded that the present CPW transmission line incorpo-

rated with a nano-granular soft magnetic film has good possibility of applications to the low-frequency pass-band filter

References

[1] Jose Carlos Pedro and Nuno Vorges Carvalho, Intermodulation Distortion in Microwave and Wireless Circuits, Artech House, Massachusetts, Chap. 2-3 (2003).
[2] Jae Cheon Sohn, Nano-granular Co-Fe-Al-O Soft Ferromagnetic Thin Films and Their Application to RF Integrated Noise Filters, Ph.D thesis, Korea University, Seoul, Chap. 2 (2005).
[3] J. C. Sohn, D. J. Byun, and S. H. Lim, J. Magn. Magn. Mater. **272-276**, 1500 (2004).
[4] J. C. Sohn, D. J. Byun, and S. H. Lim, Phys. Stat. Sol. (a) **201**(8), 1786-1789 (2004).
[5] B. C. Wadell, Transmission Line Handbook, Artech House, Massachusetts, 73-77 (1991).
[6] K. H. Kim, M. Yamaguchi, K. I. Arai, H. Nagura, and S. Ohnuma, J. Appl. Phys. **93**(10), 8002-8004 (2003).
[7] K. H. Kim, M. Yamaguchi, S. Ikeda, and K. I. Arai, IEEE Trans. Magn. **39**(5), 3031-3033 (2003).